Laboratory Studies of Al_2O_3-NO_x Aerosols

Prepared for:

U.S. Air Force Space and Missile Systems Center
Environmental Management Branch
SMC/AXFV

under
Contract F09603-95-D-0176-0007

Prepared by:

Robert Disselkamp, Ph.D.
University of Alaska Fairbanks
Geophysical Institute and Department of Chemistry
Fairbanks, Alaska

John R. Edwards
Daniel Pilson
Environmental Management Branch

Tyrrel W. Smith, Jr., Ph.D.
TRW Space & Electronics Group

Submitted by:

TRW Space & Electronics Group

30 September 1999

Report Documentation Page

Report Date	Report Type	Dates Covered (from... to)
30091999	N/A	-

Title and Subtitle Laboratory Studies of A12O3-NOx Aerosols	**Contract Number** F09603-95-D-0176-0007
	Grant Number
	Program Element Number
Author(s) Disselkamp, Robert, Edwards John R. , Pilson, Daniel, Smith, Tyrrel W.	**Project Number**
	Task Number
	Work Unit Number
Performing Organization Name(s) and Address(es) TRW and Electronics Group One Space Park, Redondo Beach, CA 90278	**Performing Organization Report Number**
Sponsoring/Monitoring Agency Name(s) and Address(es) U.S. Air Force Space and Missile Systems Center, Environmental Management Branch, El Segundo, CA	**Sponsor/Monitor's Acronym(s)** SMC/AXFV
	Sponsor/Monitor's Report Number(s)
Distribution/Availability Statement Approved for public release, distribution unlimited	
Supplementary Notes	
Abstract	
Subject Terms	
Report Classification unclassified	**Classification of this page** unclassified
Classification of Abstract unclassified	**Limitation of Abstract** UU
Number of Pages 12	

Laboratory Studies of Al_2O_3-NO_x Aerosols

Prepared for:

U.S. Air Force Space and Missile Systems Center
Environmental Management Branch
SMC/AXFV

under
Contract F09603-95-D-0176-0007

Prepared by:

Robert Disselkamp, Ph.D.
University of Alaska Fairbanks
Geophysical Institute and Department of Chemistry
Fairbanks, Alaska

John R. Edwards
Daniel Pilson
Environmental Management Branch

Tyrrel W. Smith, Jr., Ph.D.
TRW Space & Electronics Group

Submitted by:

TRW Space & Electronics Group

Approved by:

John J. Lamb, Ph.D.
Program Manager

30 September 1999

Summary of Research

Laboratory experiments have been performed to investigate chemistry in aluminum oxide (γ-Al_2O_3) aerosol samples upon exposure to NO_x (NO_x is NO, NO_2, etc.,) gases. Static aerosol samples have been generated in an aerosol chamber and studied at temperatures ranging from 298 to 183 K. Fourier-transform infrared (FTIR) absorption spectroscopy has been used to study static aerosol samples over time. Each aerosol was created using the following procedure. First, a reactant gas species, NO or NO_2, was added to the chamber and infrared spectra collected over a 20 minute time interval to characterize heterogeneous reactions occurring on the chamber walls. Next, an aluminum oxide aerosol was generated by expanding powder into the chamber using nitrogen gas at high pressure. Infrared spectra were then collected at 6 minute time intervals for at least 100 minutes to characterize Al_2O_3-NO_x chemistry. Experiments performed here enabled a quantitative characterization of both the rate of reactant gas uptake and product formation processes to be performed. A quantitative (i.e., stoichiometric) analysis of reactant gas depletion and product gas formation enabled elementary reactions involving aluminum oxide surface hydroxyl sites and NO_x species to be proposed.

Experimental Apparatus

A temperature controlled aerosol chamber capable of simulating tropospheric and stratospheric conditions has been constructed in our laboratory and is schematically illustrated in [1].

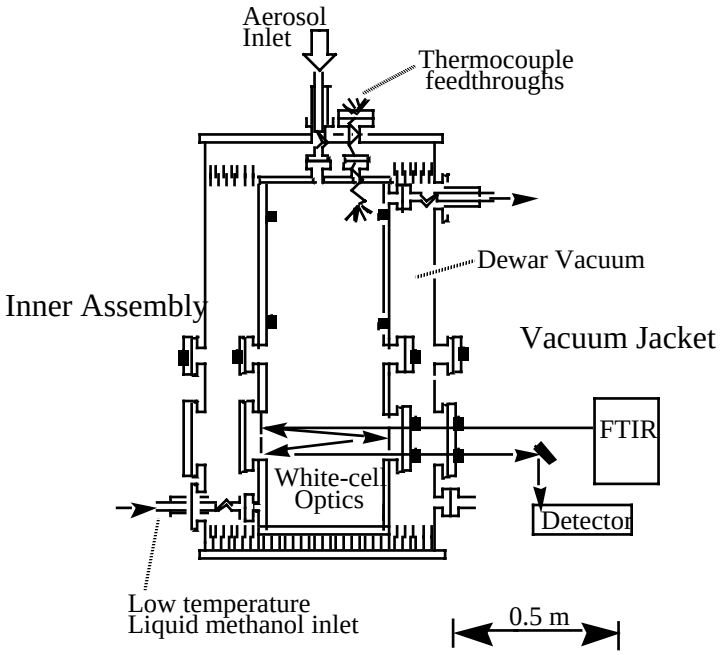

Figure 1. A schematic representation of the aerosol chamber. The inner assembl is cooled to stratospheric temperatures inside the vacuum jacket.

The chamber shown in Figure 1 is comprised of an inner assembly contained within a vacuum jacket. The vacuum jacket has been outfitted with ASA flanges, while the inner assembly contains conflat flanges compatible with temperatures as low as 77 K. The inner assembly has been thermally decoupled from its surroundings by being contained within a vacuum jacket, wrapped with ~10 layers of aluminized mylar, and stabilized by nylon supports. Temperature control of the sample region is accomplished by circulating methanol from a refrigeration unit (Neslab ULT-95) between the two concentric stainless steel cylinders of the inner assembly. The inner assembly can be cooled to any desired temperature between ambient and 183 K, with a temperature accuracy of ±1.6 K (± two standard deviations). Temperature accuracy has been determined using thermocouples located within the aerosol sample region. Five T-type thermocouple feed-throughs mounted on both the vacuum jacket and inner assembly enable thermocouple access to the sample region. The dimensions of the sample region are 18.5 cm in diameter by 105 cm in height, for a sample volume of 28 L. This volume is sufficiently large to reduce particle-wall collision events and give rise to a sufficient aerosol lifetime.

Infrared spectroscopy is a technique well-suited to probe the chemistry occurring within an aerosol sample. Collimated infrared light (Nicolet Magna-IR 560) exiting the spectrometer is focused using a pair of gold-coated first-surface plane mirrors through a pair of infrared transparent windows and into the chamber. A vacuum jacket flange is equipped with KCl salt windows, whereas an inner assembly flange contains AgCl salt windows. Two additional plane mirrors mounted within the sample region, on the inner portion of a conflat flange, are used to redirect light outside the sample region. This light is focused by an ellipsoidal mirror onto a liquid nitrogen cooled MCT-B detector element. The absorption pathlength within the sample region using this double-pass optical configuration is 32 cm. Infrared spectra from 500 cm^{-1} to 6000 cm^{-1} can be collected.

To examine the relationship between the extent of alumina hydroxylation and the rate of heterogeneous reactions, we have used an aluminum oxide cell schematically illustrated in Figure 2.

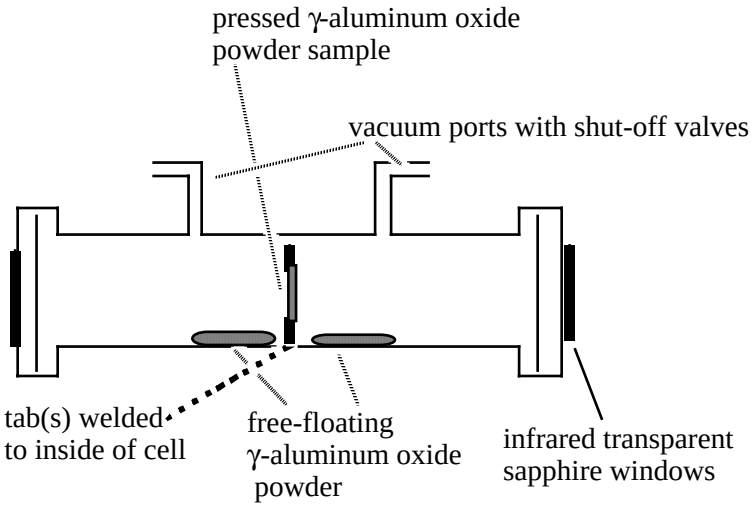

Figure 2. A schematic representation of the proposed aluminum oxide cell is shown.

The cell shown in Figure 2 is 5 inches in length and 1.5 inches in diameter. This cell is either mounted to the vacuum manifold/gas handling line of the aerosol chamber, or removed and placed into the sample accessory region of the FTIR spectrometer. Two types of alumina samples are contained within this cell: an aluminum oxide powder that has been pressed into a stainless steel wire mesh screen, and a free-floating powder in the cell. The advantage of forming a pressed sample of alumina is that extinction due to particle scattering is eliminated, thus allowing surface hydroxyl sites to be examined in the infrared at ~3800 cm^{-1}. Characterization of surface hydroxylation serves as a prelude to heterogeneous alumina aerosol experiments. In a second application, of primary interest here, the alumina is expanded into the aerosol chamber and heterogeneous chemical kinetic investigations performed.

An aluminum oxide aerosol was created using the following procedure. First, the chamber was filled with 200 Torr of filtered nitrogen gas. Next, a reagent gas was added to the gas manifold and nitrogen sent through the manifold and into the chamber, resulting in a total gas pressure of ~250 Torr. Infrared spectra collected over time enabled a characterization of heterogeneous chemistry of the NO_X reactant gas with the chamber walls. Finally, an aluminum oxide aerosol was formed using 60 psig of filtered nitrogen gas to disperse powder into the aerosol chamber. Nitrogen was flowed into the chamber until a pressure of ~1000 Torr was achieved (fill time of ~10 seconds). Infrared spectra were collected at 6 minute time intervals for 2 hours following sample preparation. The density of aluminum oxide within the chamber was readily computed by the total mass of powder used in an experiment divided by the chamber volume. A second method of determining aluminum oxide powder concentration involves the use of infrared spectroscopy to determine aluminum oxide concentration within the chamber.

The agreement between these two methods of analysis was shown to be within ±10 % [1], therefore we have used the former, and simpler, technique here.

Experimental Results

A. $NO_2/\gamma\text{-}Al_2O_3$ Aerosol Samples

The reactivity of NO_2 with γ-aluminum oxide aerosols has been characterized. Gaseous NO_2 (containing a small amount of N_2O_5) was introduced into the chamber and infrared spectra collected over a 10 minute time period to verify that its concentration was stable. Next, an aluminum oxide aerosol was created within the NO_2 sample by rapidly expanding powder into the chamber. Table 1 lists experimental conditions, such as chamber temperature, NO_2 concentration, and aluminum oxide concentrations employed. Partially dehydroxylated samples were heated to 550 K under vacuum, whereas hydroxylated samples were maintained at 300 K under vacuum prior to aerosol formation. An examination of infrared spectra of "pressed" Al_2O_3 samples have been used to determine that partially dehydroxylated samples have 20% of surface hydroxyl sites removed. An analysis of infrared spectra yielded the amount by which the reactant gas concentration is depleted during the course of an experiment, and the concentration of OH surface sites was computed from the mass of powder placed into the stainless steel cell. Using this data, the ratio of NO_2 molecules depleted to available surface sites available for adsorption was computed for each experiment. An examination of the results in Table 1 shows that only a small uptake of NO_2 occurred during each experiment performed. Furthermore, the reactivity between surface hydroxyl sites and NO_2 is very small, with increased reactivity at higher sample temperature.

The concentrations listed in Table 1 were obtained from an analysis of infrared spectra using the following procedure. The density of surface OH sites in the aerosol was computed using the equation:

$$c_{sites} = (m\, S_a\, \rho_s)/\, V \qquad (1)$$

where c_{sites} is the concentration of OH sites (sites/m^3), m is the mass of γ-Al_2O_3 (gm), S_a is the specific surface area of the powder (84 m^2/gm), ρ_s is the surface OH density (1.25×10^{19} sites/m^2) [2], and V is the volume of the chamber (0.028 m^3). The reactant gas concentration was calculated using the integrated form of the Beer's law expression,

$$c = A/\sigma\, l \qquad (2)$$

where c is the concentration of reactant gas (molecules/cm^3), A is the integrated absorbance (cm^{-1}; ν_3-band of NO_2), σ is the band strength ($5.7x10^{-17}$ cm/molecule for NO_2) [3], and l is the absorption pathlength (32 cm).

Figure 3(a) shows an infrared spectrum of a hydroxylated NO_2/Al_2O_3 aerosol at 268 K collected 2 minutes after formation. The broad feature from 500-1000 cm^{-1} is due to γ-Al_2O_3 and the intense feature at 1617 cm^{-1} is due to gaseous NO_2. Small absorption features at 1250 and 1725 cm^{-1} are due to N_2O_5. Only small changes in NO_2/N_2O_5 absorption were observed over 120 minutes. To quantify NO_2 gas depletion we have computed a difference spectrum. Figure 3(b) is the difference spectrum obtained from a spectrum obtained at 2 minutes minus a spectrum obtained at 120 minutes. Figure 3(b) shows a noticeable, but small, decrease in Al_2O_3, NO_2, and N_2O_5 absorbencies. Aluminum oxide powder disappearance is due to aerosol particle sedimentation out of the optical interrogation region, whereas NO_2/N_2O_5 disappearance is likely due to chemistry. The NO_2/N_2O_5 concentrations were reduced by 2.1% during the course of this experiment. A full analysis of this experiment is contained in the first column listed in Table 1.

A similar experimental approach has been used to investigate hydroxylated NO_2/γ-Al_2O_3 aerosols. Figure 4 shows an infrared spectrum collected for a hydroxylated aerosol at a chamber temperature of 223 K. An analysis of this experiment is listed as the third column in Table 1. Figure 4(a) was collected 2 minutes after aerosol formation and reveals NO_2, N_2O_5, and γ-Al_2O_3 absorption features. Note that the N_2O_5:NO_2 absorption feature ratio is significantly larger than that in Figure 3(a), presumably due to a shift in NO_2/N_2O_5 equilibrium at the lower chamber temperature employed [4]. (An impurity explanation has been ruled out due since this gas partitioning is reproducible.) Since oxygen (O_2(g)) was not introduced into any of our aerosol samples, we can speculate that the chamber walls provide a source of oxygen to form N_2O_5 from NO_2. The difference spectrum of Figure 4(b) minus Figure 4(a) has been used to compute NO_2 uptake and is listed as the third column of Table 1. Only 0.24% of NO_2 was depleted during the course of this experiment. The relative NO_2 to N_2O_5 absorption ratio is preserved in the difference spectrum of Figure 4(b), consistent with an equilibrium relationship between NO_2/N_2O_5.

B. NO/γ-Al_2O_3 Aerosol Samples at 298 K

Nitric oxide/γ-Al_2O_3 aerosol samples exhibit interesting and complex chemistry. Figure 5 presents infrared spectra of a partially dehydroxylated NO/γ-Al_2O_3 aerosol at 298 K. The spectrum in Figure 5(a) was collected 2 minutes after aerosol formation, whereas the spectrum in Figure 5(b) was collected 100 minutes after aerosol formation. These spectra reveal a dramatic

increase in NO_2 absorption and a decrease in NO absorption. A photometric (i.e., quantitative) analysis confirmed that NO was converted into NO_2 with unity efficiency. This was accomplished by noting that the band cross-section of NO_2 [3] is a factor of 26 larger than that of NO (σ=2.17x10^{-18} cm/molecule) [5]. An examination of the conversion of NO to NO_2 due to chamber wall processes was performed just prior to each aerosol experiment and revealed a much slower conversion of NO to NO_2. For example, the experiment here revealed an NO absorption intensity decreasing of only 8 % over a 100 minute time period. Similar results were obtained for a hydroxylated aerosol experiment performed at 298 K. Figure 6 presents infrared spectra for a hydroxylated aerosol collected at (a) 2 minutes, and (b) 100 minutes, after aerosol formation. Again an efficient conversion of NO to NO_2 was observed, with the chamber wall process (measured just prior to the aerosol experiment) converting only 6% of NO to NO_2 over the same time period. An analysis of these two experiments is presented in the two left-hand columns of Table 2, and include initial NO concentration, NO_2 produced, and hydroxyl surface site concentration.

A summary of the time evolution of the dehydroxylated/hydroxylated NO/γ-Al_2O_3 aerosol experiments at 298 K is presented in Figure 7. The symbols illustrate NO_2 (blackened) and NO (non-blackened) concentrations determined from infrared spectra and a photometric analysis. Based on a quantitative analysis of the conversion of NO to NO_2, we propose the following reaction sequence to account for the observed chemistry.

$$NO + Al\text{-}(OH)\text{-}Al\text{-}(OH) \rightarrow NO_2 + H_2O + Al\text{-}()\text{-}Al\text{-}() \quad (3)$$

$$2\ NO + Al\text{-}()\text{-}Al\text{-}() \rightarrow Al\text{-}(NO)\text{-}Al\text{-}(NO) \quad (4)$$

Reaction (3) describes the reaction of a nitric oxide species with two surface hydroxyl groups to form NO_2 and H_2O. The variability of H_2O absorption arising from purging fluctuations did not enable water formation to be observed. Reaction (4) is a subsequent reaction of two nitric oxide species with the bare (dehydroxylated) aluminum oxide surface sites. The combined two reactions describe the conversion of 3 NO species into one NO_2, one H_2O, and two surface NO species adsorbed onto γ-Al_2O_3. The feasibility of the reaction stoichiometry proposed here can be evaluated using experimental results contained in Figure 7 and in Table 2 (see the bottom two entries in Table 2). The first step in examining the viability of reactions (2) and (3) is identifying the limiting reagent. Since [OH]=2.6x10^{16} sites/cm^3 and the initial [NO]>8x10^{16} molecules/cm^3, and three NO can reaction with two OH sites, the limiting reagent is the hydroxyl site concentration. Based on the initial hydroxyl site concentration, roughly (3/2) x 2.6x10^{16}, or

3.9×10^{16} NO species/cm^3 are expected to be depleted in each aerosol experiment. This value is close to that observed of 4.0×10^{16} and 5.7×10^{16} NO species/cm^3 for the dehydroxylated and hydroxylated aerosol experiments, respectively. Furthermore, according to reactions (3) and (4), the stoichiometric ratio of NO depleted to NO_2 formed is expected to be 3.0. The observed values of 2.1 and 2.3 for the hydroxylated and dehydroxylated experiments are again close to that observed. It can be concluded that NO undergoes rapid reaction with hydroxyl groups on the surface of γ-Al_2O_3. The greater reactivity in NO/γ-Al_2O_3 versus NO_2/γ-Al_2O_3 aerosols is not surprising, since the heat of formation (ΔH_f) of NO of 21.6 kcal/mol is much greater than that of 7.6 kcal/mol for NO_2 [6].

C. NO/γ-Al_2O_3 Aerosol Samples at 183 K

Nitric oxide/γ-Al_2O_3 aerosol experiments at 183 K exhibited more complex chemistry than the corresponding studies at 298 K. Figure 8 presents infrared spectra of a nitric oxide gaseous sample placed into the chamber, in the absence of a γ-Al_2O_3 aerosol, and infrared spectra collected at (a) 2 minutes and (b) 120 minutes after sample formation. An examination of these infrared spectra can be used to characterize chemistry occurring on the inside walls of the aerosol chamber at 183 K. A number of observations can be noted from an examination of the variation in absorption intensity over time. First, a 5-fold reduction in concentration of NO and NO_2 took place (final NO and NO_2 concentrations were 14% and 18% of original values, respectively). Second, a 160% increase in N_2O_5 concentration occurred, whereas only a 125% increase in N_2O took place. Although it is difficult to make any definitive statement about these concentration changes inferred from integrated absorption changes, a reaction that accounts for this chemistry is

$$NO + NO_2 + Fe_2O_3 \rightarrow N_2O_5 + FeO. \qquad (5)$$

Combining reaction (5) with reactions (3) and (4) above suggests that the chamber walls catalyze the conversion of NO to NO_2, and at low temperature reaction (5) results in N_2O_5 formation. The question then arises as to whether γ-Al_2O_3 enhances this chemical conversion of NO to N_2O_5.

Figure 9 presents results of a hydroxylated NO/γ-Al_2O_3 aerosol at 183 K. Again spectra were obtained (a) 2 minutes and (b) 120 minutes after aerosol formation. The change in reactant gas concentration is seen to be different than that presented in Figure 8 for the NO reactant gas-only experiment. In Figure 9 the NO, NO_2, and N_2O_5 concentrations decrease to 6%, 10%, and 30% of their original values, whereas the N_2O concentration undergoes a modest increase of 9%. The unexpected result, based on our discussion above of the NO reactant gas data, is the decrease

in N_2O_5 concentration. Since the presence of γ-Al_2O_3 will not inhibit wall reaction processes, we propose that N_2O_5 uptake onto the aluminum oxide surface occurs. A likely reaction sequence for this uptake is surface adsorption, followed by hydrolysis of N_2O_5 to form nitric acid on the surface of aluminum oxide. Similar results were observed for a dehydroxylated NO/γ-Al_2O_3 aerosol sample. Figure 10 presents infrared spectra collected at (a) 2 minutes and (b) 120 minutes after aerosol formation. Again NO, NO_2, and N_2O_5 absorption's decrease with time. However in this dehydroxylated experiment the decrease in NO concentration during the 118 minute reaction time is 57%, much smaller than the decrease to 6% of original concentrations (t=2 minutes) observed for the hydroxylated aerosol. A decrease in the surface water content for the partially dehydroxylated γ-Al_2O_3 aerosol may be the cause of this reduced NO conversion to NO_2/N_2O_5.

Stratospheric Implications

The uptake of NO onto the surface of γ-Al_2O_3 has two potential implications in atmospheric chemistry. First, a decrease in atmospheric NO_x concentrations can enhance the catalytic destruction of ozone by halogen species. To investigate whether this would be a likely process in the stratosphere consider that a single 1 μm size aluminum oxide particle has a surface area of 3.2×10^{-8} cm^2. Since the hydroxyl site density is 1.3×10^{15} OH species/cm^2 [2], and each OH site can accommodate one NO species, then the uptake of NO species is 3.9×10^7 NO species/particle. Considering that the ambient NO_x concentration is 10 ppb, or 2.5×10^{10} molecules/cm^3, it would take a particle density of 640 particles/cm^3 to deplete all the NO_x species. It can be concluded that within the wake of rocket exhaust plume this chemistry may be important, but not at the aluminum oxide ambient particle concentration of ~10 particles/m^3. A second potential atmospheric implication of this chemistry is the uptake of halogen species onto the surface of aluminum oxide particles. For example, a reaction that may occur is

$$Cl_y + \text{Al-OH} \rightarrow \text{Al-Cl} + OH^{\cdot} \qquad (6)$$

The uptake of active halogen species by aluminum oxide to liberate NO would have the effect of increasing the ozone concentration by reducing the contribution of halogen catalyzed ozone destruction. Additional studies are needed to characterize this halogen chemistry.

Table 1. Analysis of Al_2O_3 Aerosol Samples with NO_2

Reactant gas:	NO_2			
Temperature:	268 K	290 K	223 K	223 K
Aerosol:	hydroxylated	dehydroxylated	hydroxylated	dehydroxylated
Initial NO_2 concentration[a]	1.2×10^{16}	2.3×10^{16}	3.5×10^{15}	2.1×10^{15}
NO_2 depleted at 120 minutes[a]	2.6×10^{14}	1.4×10^{15}	8.4×10^{12}	1.8×10^{13}
NO_2 depleted (%)[a]	2.1	6.4	0.24	0.9
OH Site concentration[a]	2.6×10^{16}	2.7×10^{16}	2.6×10^{16}	2.4×10^{16}
Depleted NO_2 per Total Sites (%)	1.0	5.3	0.032	0.075

[a] Concentrations given in units of molecules/cm^3.

Table 2. Analysis of Al_2O_3 Aerosol Samples with NO

Reactant gas:	NO			
Temperature:	298 K	298 K	183 K	183 K
Aerosol:	dehydroxylated	hydroxylated	hydroxylated	dehydroxylated
Initial NO concentration[a]	8.8×10^{16}	1.1×10^{17}	3.5×10^{15}	2.1×10^{15}
NO_2 formed at 100 minutes[a]	1.9×10^{16}	3.1×10^{16}	8.4×10^{12}	1.8×10^{13}
OH Site concentration[a]	2.6×10^{16}	2.6×10^{16}	0.24	0.9
[NO] depletion/[NO_2] formation	2.3	2.1	2.6×10^{16}	2.4×10^{16}
Depleted NO[a]	4.0×10^{16}	5.7×10^{16}	0.032	0.075

[a] Concentrations given in units of molecules/cm^3.

References

1. M.L. Narus, N.C. Schoenfelder, Y. Na., L.A. Chavasse, R.S. Disselkamp, *A Chamber for Laboratory Studies of Atmospheric Aerosols and Clouds*, Rev. Sci. Instr., **67**, 4364 (1996).

2. J.B. Peri, *Infrared and Gravimetric Study of Surface Hydration of γ-Alumina*, J. Phys. Chem., **69**, 211 (1965).

3. Camy-Peyret, C., J.-M. Flaud, A. Perrin, 1982: Improved Line Parameters for the ν_3 and $\nu_2+\nu_3-\nu_2$ Bands of $^{14}N^{16}O_2$, J. Mol. Spect., **95**, 72-79.

4. Cantrell, C.A., J.A. Davidson, A.H. McDaniel, R.E. Shetter, J.G. Calvert, 1988: Infrared Absorption Cross Sections for Nitrogen Pentoxide (N_2O_5), Chem. Phys. Lett., **148**, 358-363.

5. Falcone, P.K., R.K. Hanson, C.H. Kruger, J. Quant. Spectrosc. Rad. Trans., **29**, 205 (1983).

6. Benson, S., *Thermochemical Kinetics, Methods for the Estimation of Thermochemical Data and Rate Parameters*, Second ed., John Wiley & Sons Inc., 1976.